SINGULAR VALUE DECOMPOSITION FOR COMPRESSION OF LARGE-SCALE RADIO FREQUENCY SIGNALS

R. David Badger[1,2], Minje Kim[1]
[1]Indiana University, Department of Intelligent Systems Engineering, Bloomington, IN, USA 47408
[2]Naval Surface Warfare Center Crane, Crane, IN, USA, 47522
rdbadger@iu.edu, minje@indiana.edu

***Abstract*—The paper proposes an efficient matrix factorization-based approach to large-scale radio frequency (RF) signal compression tasks. While data compression techniques can significantly reduce the storage requirements and memory bandwidths for many types of data including image and audio files, a reasonable implementation for RF signals is less explored. However, since recorded RF signals can be extremely large, they often significantly impact the storage and handling of the data. In this paper, we focus on software defined radios (SDR) that process RF signals in the in-phase (I) and quadrature (Q) time samples, which are then transformed into a time-frequency representation. We investigate the use cases of the singular value decomposition (SVD) algorithm, which reduces the dimension of the time-frequency representation of the IQ samples, forming a low-rank approximation of the original. We validate the proposed method in various lossy RF signal compression tasks that show fast and reliable compression results with acceptable reconstruction error.**

***Index Terms*—Radio Frequency (RF), Singular Value Decomposition (SVD), Software Defined Radio (SDR), Universal Software Radio Peripheral (USRP), Short-Time Fourier Transform (STFT), In-phase and quadrature (IQ)**

I. Introduction

Monitoring and collecting Radio Frequency (RF) data has become an important part of spectrum management as RF electromagnetic waves permeate almost every facet of our lives. Cellular telephones, Wi-Fi, radio stations, satellites, and garage door openers all use the RF signals to transmit and receive information. It is often accomplished through the use of the software defined radio (SDR) [1], [2]. SDRs are an inexpensive and convenient way to collect RF signals, real-time spectrum monitoring, and as a software transceiver for RF communication. SDR hardware is simplified compared to specific application transceivers because SDR hardware is used to sample the spectrum or transmit the in-phase and quadrature (IQ) format, typically without any additional hardware processing. The IQ stream is transferred to a host computer where software can store the IQ data or function as a transceiver for signal processing [3] [4].

Existing methods for IQ compression are primarily used within RF communication equipment that is transferring the IQ data on internal buses. This type of IQ compression reduces buss bandwidth requirements through decimation/down-sampling, and is often in the time domain with a typical compression of four [5]. This is different from research presented here in that our proposed compression method is defined in the frequency domain and works in an offline manner, thus resulting in a significantly greater compression ratio.

Our methods works on the time-frequency (TF) representation of an originally IQ formatted RF data. For a given discrete-time waveform signal,

$$x(n) = \sin(2\pi f n + \phi(n)), \tag{1}$$

where f, n and $\phi(n)$ are for the frequency and time indices, and time-varying phase shifts, respectively. Then, trigonometry can represent (1) as the sum of the orthogonal components:

$$\text{In-Phase} \quad i(n) = \sin(2\pi f n)\cos(\phi(n)) \tag{2}$$

$$\text{Quadrature} \quad q(n) = \sin\left(2\pi f n + \frac{\pi}{2}\right)\sin(\phi(n)). \tag{3}$$

While collecting and archiving RF data have many uses, IQ samples can generate very large files, depending on bandwidth and duration of collection. For example, IQ sample files can range from 40MB at 1 mega samples per second (MSPS) to over 1GB at 25MSPS for each collect of five seconds.

Our goal is to compress this kind of data without loss of critical information to actuate the matched receiver. One way to achieve the reduction of data rate is to quantize the signal using a low bit-depth. In [6], the TF domain is sub-divided into multiple groups of subbands and quantized separately. Coupled with a thresholding technique that suppresses lower magnitudes, this method achieves a reasonable compression ratio. However, our proposed low-rank approximation-based approach is orthogonal to the quantization mechanism, making the two approaches complementary to each other.

Meanwhile, in [7], robust principal component analysis (RPCA) is used to remove unwanted interference from the RF signal in the TF domain. Given that RPCA is based on the low-rank approximation of the signals, this approach shares the same philosophy with ours. However, its experimental design is focused on interference suppression than compression performance. Our work presents a singular vector decomposition (SVD)-based algorithm [8] to substitute the time-frequency representation of the IQ data with a low-rank approximation. We also presents the compression performance on various analogue and digital RF signals.

Furthermore, we are also interested in investigation of the use of graphics processing units (GPU) for the time-frequency transformation and SVD implementations to see if parallel processing can expedite those processes. The SVD algorithm was fully supported in PyTorch version 1.6.

There are two different cases of reconstructed IQ data to consider: the analog and digital cases. First, as for the analog push-to-talk (PTT) transceivers, for example, if reconstruction can actuate the matched receiver without any perceivable degradation in speech quality, it can be considered to be a *good* reconstruction, and vice versa. We will discuss more about the subjectivity of speech quality measurements in Section V-C. The second case is the digital transceivers, where the bit error rate (BER) can monitor the reconstruction efficacy. However, the procedure proposed by Mitra [9] was not feasible for us due to the lack of transceiver's physical layer architecture, schematic diagram of signal path, and equipment to measure BER. Instead, we assume that if the reconstructed signal can reliably actuate the transceiver with a high probability, the internal BER at the receiver must be lower than maximum allowable value. Further empirical measures of the reconstructed IQ signals are discussed in Section V-B.

We claim that this work is the first attempt to compress RF signals using the well-defined low-rank approximation concept, achieving a sensible compression ratio to the best of our knowledge. The lack of a compression method in the literature might be due to the communication-oriented nature of the RF signal processing domain, where RF signals are not considered as stored data to be compressed, although we have been motivated by this problem from our practice. While SVD itself has been widely studied in the literature, we fully utilized it in the time-frequency domain. Eventually, one can control the tradeoff between the compression ratio and reconstruction quality based on the orthogonality of SVD.

II. Background

We convert the IQ data into the time-frequency domain with a short-time Fourier transform (STFT) function [10]. The discrete STFT of a discrete time signal $x(n)$ with a symmetric, typically bell-shaped window function $\omega(t)$ of length H (i.e., the number of consecutive non-zero elements) is defined as:

$$\mathrm{STFT}\{x(n)\}(f,t) \equiv \boldsymbol{X}_{f,t} = \sum_{n=-\infty}^{\infty} x(n)\omega(n-tR)e^{-j2\pi fn}, \tag{4}$$

where t and R denote the frame index and hop size, respectively. STFT results in a complex matrix $\boldsymbol{X}$. We expand this operation to both I and Q channels, to convert the time-domain signals $i(n)$ and $q(n)$ into $\boldsymbol{I}$ and $\boldsymbol{Q} \in \mathbb{C}^{F\times T}$, where F and T are the number of frequency subbands and frames, respectively. The size of this complex matrix is defined by the bandwidth of the signal as well as the frame rate, i.e., the hop size between the windowed frames, which we set to be 50% of the frame size. Inverse of the STFT (iSTFT) is defined by applying inverse DFT to each spectrum $\boldsymbol{X}_{:,t}$, which recovers the windowed time domain signal $x(n)\omega(n-tR)$. An overlap-and-add process follows to recover the original $x(n)$ based on the constant overlap-and-add property of the window function.

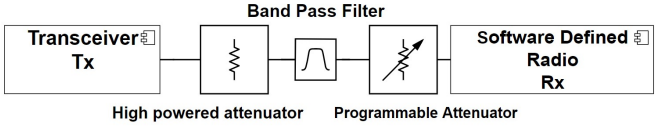

Fig. 1. The closed loop coaxial setup.

Meanwhile, SVD factorizes a given matrix $A \in \mathbb{R}^{M\times N}$ into three factor matrices, $\boldsymbol{A} = \boldsymbol{U}\boldsymbol{\Sigma}\boldsymbol{V}^\top$, where $\boldsymbol{U}$ and $\boldsymbol{V}$ hold orthonormal basis vectors whose significance is represented by the corresponding singular values, stored in the diagonal matrix $\boldsymbol{\Sigma}$. SVD has been used for compressing images for over forty years [11], [12]. The compression relies on the assumption that the rank K of the input matrix $\boldsymbol{A}$ is lower than its dimensions, i.e., $K < M, N$, which is defined as the number of non-zero singular values. In practice, as we do not know the exact rank due to the noisy nature of the data, one can choose a reasonable rank $L < M, N$ with a risk of reconstructing a rank-deficient version of the input:

$$\boldsymbol{A} = \boldsymbol{U}\boldsymbol{\Sigma}\boldsymbol{V}^\top \approx \hat{\boldsymbol{A}}^{(L)} = \sum_{k=1}^{L} \boldsymbol{U}_{:,k}\boldsymbol{\Sigma}_{k,k}\boldsymbol{V}_{:,k}^\top. \tag{5}$$

These applications are similar to our approach, in the sense that STFT converts the IQ stream into arrays. For example, by taking the magnitude of the STFT, we can visualize the TF representation as an image as shown in the figures in this paper. However, our method applies SVD to all real and imaginary coefficients instead of the magnitudes in order to re-constitute them into IQ data without losing the phase information.

III. Data Preparation: SDR and SigMF

This work used GNU Radio (`gnuradio`) [13] to collect RF waveforms for analysis and transformation. Within `gnuradio`, an additional out-of-tree (OOT) module was used during signal collection. This module facilitated the collection of IQ data as well as labeled metadata in the format compatible to SigMF [14]. All data were collected at the sampling rate of 1 MSPS producing a bandwidth of 1MHz. The signal duration was 5 seconds for the results sections V-A, V-B, and V-D and 15 seconds for the efficacy calculations section V-C. The transceivers operated at or around the 433 MHz, the industrial, scientific, and medical (ISM) band. IQ data was recorded using an Ettus N210 SDR with SBX daughter board. Data was transferred over-the-wire between the SDR and CPU as a complex 16bit integer [15]. The CPU converted the data to 32 bit float for use in `gnuradio` applications.

Two methods were used to connect the transmitted waveform to the matched receiver: closed-loop and OTA. The former is to represent the setup where interference from outside source is minimized. OTA, on the other hand, relies on the antennas, leading to a higher probability of signals of non-interest getting recorded.

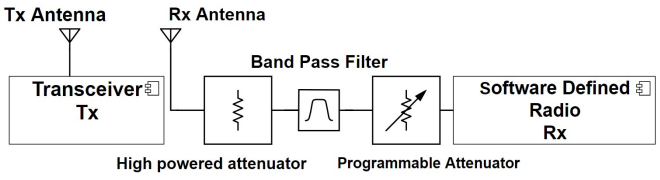

Fig. 2. Over the air coaxial setup

Closed loop setup: The closed loop setup connects the Tx directly to the Rx through a coaxial network. The basic closed loop and OTA configuration consisted of a high powered 30dB attenuator inserted from the Tx output, in-line with an 8 MHz band-pass filter centered at 433 MHz. It was followed by a Mini-Circuits' VLM-33-2W+ coaxial RF limiter to protect the programmable attenuator and SDR from high-powered signals. The final component before the input to the programmable attenuator was a Mini-Circuits' BLK89-S+ DC-Block, to prevent DC power getting into the front end of the attenuator and SDR. All transmitters were properly attenuated to ensure high SNR at the receiver, while also ensuring recorded signals stayed in the linear region of the receiver. Fig. 1 depicts a simplified schematic of the RF hardware setup for closed loop collection.

OTA setup: OTA collection was performed for Tx that did not have a removable antenna or was not easily configurable for the closed-loop setup. Fig. 2 illustrates a simplified schematic of the OTA setup. The primary difference between the two configurations is the use of antennas for waveform propagation. The OTA method featured Tx and Rx antennas that were optimized for the operating frequencies. The physical distance between the Tx and the Rx antennas was 2λ ($\lambda = wavelength$) or more to ensure the Rx was in the far field when recording IQ signals. An 8 MHz bandpass filter was also applied.

SDR transmission: Transmitting a recorded IQ file via SDR will actuate a matched receiver, as if it had been sent by the original transmitter with minimal added artifacts. However, we feed the IQ data to our compression and decompression pipeline, i.e., STFT—low rank SVD—iSTFT, which replaces the original IQ data with a low rank approximation. The SVD was performed on a computer using the saved IQ data, then a new IQ file was reconstructed from the reduced rank matrix. Fig. 2 depicted the typical transceiver to SDR setup. When recording IQ files, the path was from the transceiver to the SDR. After reconstructing a waveform, the transmission path was from the SDR to the transceiver.

The authors made the IQ datasets and the python code used to analyze the data publicly available[1].

IV. STFT and SVD for Compression

We used EVGA® GTX1080Ti (3584 NVIDIA® CUDA® cores) to run PyTorch 1.6's STFT and iSTFT algorithms (`torch.stft` and `torch.istft`). While CPU implementations are also an option, both algorithms were, on average, 12.5 times faster on the GPU. STFT and iSTFT used a frame size of 1024 samples and a 50% of overlap. Each frame is windowed by a Hann window of the same size. The frequency dimension is $F = 513$ (due to the complex conjugacy we discard about a half of the frequency dimensions), resulting in the frequency resolution at 976.56 Hz. This granularity was chosen due to the amount of GPU memory required to perform matrix operations, while it was sufficient to activate matched receivers during the low rank SVD reconstitution. The number of frames T varies depending on the length of the signal. We apply STFT to each of the I and Q channels, respectively, which results in four real-valued spectrograms, $\boldsymbol{I}^{(\text{Real})}$, $\boldsymbol{I}^{(\text{Imag})}$, $\boldsymbol{Q}^{(\text{Real})}$, and $\boldsymbol{Q}^{(\text{Imag})}$:

$$\text{STFT}\{i(n)\} \equiv \boldsymbol{I}^{(\text{Real})} + j\boldsymbol{I}^{(\text{Imag})} \tag{6}$$

$$\text{STFT}\{q(n)\} \equiv \boldsymbol{Q}^{(\text{Real})} + j\boldsymbol{Q}^{(\text{Imag})} \tag{7}$$

PyTorch implementation of the SVD algorithm is applied to each of the four spectrograms, respectively. As our compression ratio depends on the choice of rank L, we performed a simple test to choose a small enough, but working value. To this end, SVD was performed on select recorded IQ waveforms. All selected IQ files were verified to trigger the associated receiver using SDR playback. After factorization occurred, each waveform was reconstructed with a varying amount of singular vectors L. Once the waveform was reconstructed via iSTFT, it was re-transmitted OTA and tested to see if the matched receiver could successfully demodulate the reconstructed signal. Fig. 3 depicts the relationship between the chosen rank L and the Euclidean norm ratio in per cent error, $\mathcal{E}(L) = \left(\sum_{f,t}\left(\boldsymbol{A}_{ft} - \hat{\boldsymbol{A}}_{ft}^{(L)}\right)^2\right)^{1/2} \Big/ \left(\sum_{f,t}\boldsymbol{A}_{ft}^2\right)^{1/2}$.

V. Experimental Results

Our experiments are designed to empirically verify that the proposed low-rank approximation can actuate the receiver with a significantly lower amount of bits. However, note that its data-driven nature limits our ability to prove the performance guarantee. Our fundamental assumption is that the rank of the RF signals' time-frequency representation may be lower than their actual dimensions as in many other signal domains (e.g., audio and video), while the actual working rank can be found only empirically. Our SVD-based approach supports this search, as SVD's orthogonality lets the user incrementally add additional latent variables until a satisfying reconstruction quality is achieved (the "elbow" method shown in Fig. 3).

A. Analog waveforms: PTT radio

The Baofeng UV5R analog PTT radios used in this paper use a frequency modulation (FM) waveform and were relatively easy to reproduce from a low rank approximation due to receiver design. Presenting enough in-channel energy to break squelch, the analog receiver chain demodulated the signal.

$L = 3$ was the minimum rank to actuate the PTT receiver and be intelligible, while it introduced noticeable audio artifact.

[1]https://saige.sice.indiana.edu/research-projects/rf-svd

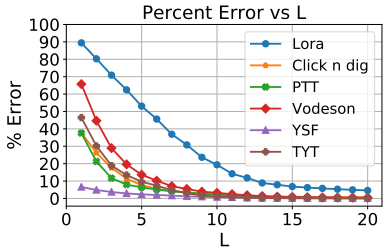

Fig. 3. The reconstruction percent error by varying choices of L.

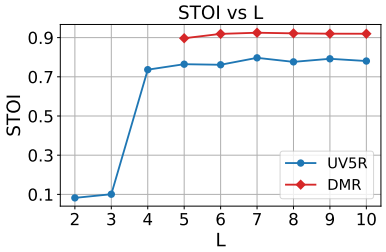

Fig. 4. The speech intelligibility potential of the low rank approximation.

TABLE I
THE RANK VALUES THAT MEETS CERTAIN PERCENT ERROR THRESHOLDS, 5% AND 1% ERROR.

Rank (Percent Error)	L ($<$ 5%)	L ($<$ 1%)
PTT	7 (4.13%)	14 (0.78%)
TYT®	7 (4.82%)	11 (0.80%)
Vodeson	9 (3.90%)	15 (0.84%)
Click 'n Dig®	7 (4.23%)	15 (0.95%)
YSF	2 (4.86%)	10 (0.79%)
LoRa™	19 (4.83%)	104 (0.99%)

With four vectors, the sound quality was perceptually indistinguishable from the uncompressed original. Corresponding ranks for 5% and 1% errors were $L = 6$ and $L = 15$, respectively. Fig. 5 zooms into the details of spectral changes as L increases. Note that figures 5 and 6 are frequency components in the Y-axis, as FFT bins. We can see that the full rank approximation recovers most of the details, while $L = 15$ also captures an important structure. A more detailed analysis on the audio quality is discussed in Section V-C.

B. Digital waveforms

Five different transceiver models were investigated for the digital setup:

- TYT® DMR radio: A digital mobile radio (DMR) that uses 4FSK modulation and 30 msec time division multiple access (TDMA) channels.
- Vodeson HD03 Doorbell: Operates in the 434 MHz band.
- Click 'n Dig® D2 FOB: Operates in the 434 MHz band.
- Yaesu System Fusion (YSF) C4FM: YSF has four modes of operation, one analog and three digital C4FM modes. The results published here are the voice full-rate mode [16]. In this mode the entire 12.5 kHz bandwidth was used.
- LoRa™ FMCW or CSS: It is a frequency modulated continuous wave (FMCW) / chirp spread spectrum (CSS) waveform [17]. The tested configuration for LoRa™ was a HopeRF RFM98 module [18] with a spreading factor of 9 and bandwidth of 125 kHz.

In Fig. 3 and Table I we can see that significantly small values for L, less than 10 most of the time, can recover 95% of the original matrix in terms of the Euclidean norm ratio. For a higher reconstruction quality of 99%, more ranks are required, but not exceeding 15 most of the time. Meanwhile, LoRa™ is the most difficult case that requires substantially higher ranks, which is due to its complex zigzag pattern in the time-frequency domain shown in Fig. 6.

A significant difference that distinguishes digital modulation from analog is that analog receivers will generally break squelch and activate the receiver; if the signal has enough of the proper modulation characteristics, then poor to excellent communication can be achieved. On the other hand, in order to activate digital receivers enough packets or symbols have to be received and properly demodulated. This means that the actuation of receivers can indirectly determine the quality of the reconstruction, which is generally the case for all digital modulation experiments. All modulations were initiated with a small L; the minimum is reported in Table II.

C. Signal reconstruction efficacy for voice communication

We employ short-time objective intelligibility (STOI) measures [19] to empirically determine the quality of received IQ voice transmissions for select analog and digital PTT waveforms. A ten second voice file from the LibriSpeech corpus [20] was played by a loudspeaker, which the Tx unit captured. The RF waveform was captured using the OTA setup depicted in Fig. 2. After performing SVD, the recovered IQ signal is transmitted to the original receiver, which extracts the speech signal and plays it using its own loudspeaker.

The audio recording process creates some additional artifact, which we minimize by keeping the microphone and PTT speaker's physical orientation constant. The received signal is temporally aligned to the playback of the Rx that did not go through the compression process, by using their cross-correlation. The STOI measurements in Fig. 4 for the Baofeng UV5R analog PTT transceiver coincides with listening to the audio signals: after about five vectors, it was hard to hear an increase in audio quality. The digital TYT® MD-380 DMR waveform was reconstituted and triggered the matched receiver with as few as five vectors. The sound quality was digitally clear and no improvement was audible as L increased, which explains the STOI values that saturate at $L = 5$.

D. Compression Analysis

Actual compression ratios can be calculated based on original IQ data size divided by the sum of the saved arrays' file size. For a given windowed frame of size H, FFT gives $2H$ real and imaginary coefficients; half of them will be kept due to the complex conjugacy. Since the 50% overlap doubles the frame rate, STFT ends up with twice more coefficients, i.e., $FT = 2J$ for a signal with J samples. Meanwhile, when $L < F, T$, the compression ratio is $(FT/2)/(FL + L + LT)$, which is in the order of $\mathcal{O}\big((FT)/(F + T)\big)$ when $L \ll F, T$.

VI. Conclusion

In this research, electromagnetic waves were sampled with SDRs. The SVD algorithm was successfully employed to reduce the vectors necessary to re-constitute, transmit, and

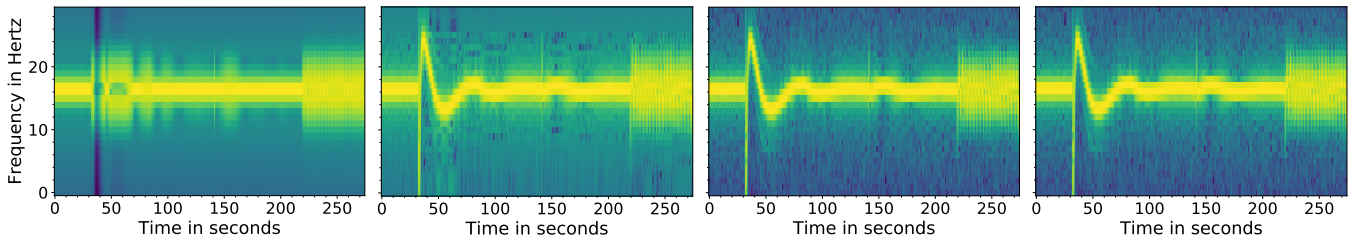

(a) $L = 2$ (b) $L = 15$ (c) $L = 1024$ (d) Original

Fig. 5. The reconstructed PTT spectrograms with varying ranks.

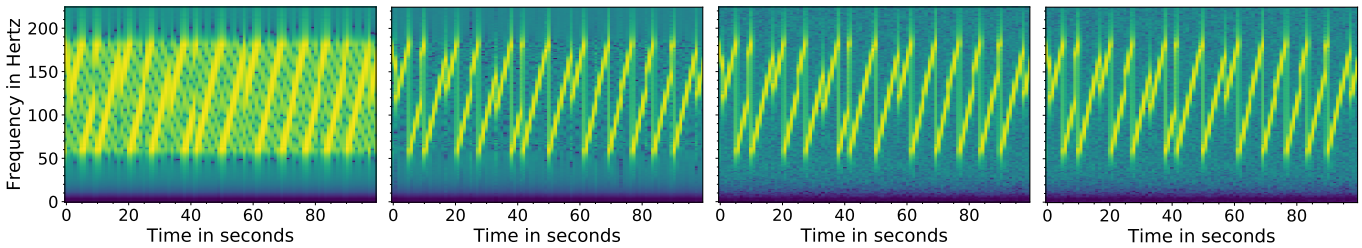

(a) $L = 5$ (b) $L = 30$ (c) $L = 1024$ (d) Original

Fig. 6. The reconstructed LoRa™ spectrograms with varying ranks.

TABLE II
COMPRESSION ANALYSIS. MINIMUM L INDICATES THE MINIMUM RANK REQUIRED TO ACTUATE THE RECEIVER.

Modulation	Compression Ratio	Actual L	Minimum L
PTT	24.57	10	2
TYT®	24.27	10	5
Vodeson	121.01	2	2
Click 'n Dig®	34.69	7	7
YSF	40.48	6	6
LoRa™	8.64	28	28

activate the matched receiver. This reduced the required vectors down to 0.2 - 2.8 percent of the original vectors, and provided data compression ratios from about 8.64 to 121. The compression ratios achieved can significantly reduce storage and handling of RF IQ data.

REFERENCES

[1] J. Mitola, "The software radio architecture," *IEEE Communications Magazine*, vol. 33, no. 5, pp. 26–38, 1995.

[2] R. Bagheri, A. Mirzaei, M. E. Heidari, S. Chehrazi, M. Lee, M. Mikhemar, W. K. Tang, and A. A. Abidi, "Software-defined radio receiver: dream to reality," *IEEE Communications Magazine*, vol. 44, no. 8, pp. 111–118, 2006.

[3] W. H. Tuttlebee, *Software defined radio: enabling technologies*. John Wiley & Sons, 2003.

[4] A. M. Wyglinski, D. P. Orofino, M. N. Ettus, and T. W. Rondeau, "Revolutionizing software defined radio: case studies in hardware, software, and education," *IEEE Communications Magazine*, vol. 54, no. 1, pp. 68–75, 2016.

[5] J. Lee, E. Hyun, and J.-Y. Jung, "A simple and efficient IQ data compression method based on latency, evm, and compression ratio analysis," *IEEE Access*, vol. PP, pp. 1–1, Aug. 2019.

[6] D. Muir, L. H. Crockett, and R. W. Stewart, "Generic compression of off-the-air radio frequency signals with grouped-bin FFT quantisation," in *28th European Signal Processing Conference (EUSIPCO)*, 2020, pp. 1767–1771.

[7] L. H. Nguyen and T. D. Tran, "RFI-radar signal separation via simultaneous low-rank and sparse recovery," in *2016 IEEE Radar Conference (RadarConf)*, 2016, pp. 1–5.

[8] G. W. Stewart, "On the early history of the singular value decomposition," *SIAM Review*, vol. 35, no. 4, pp. 551–566, 1993. [Online]. Available: https://doi.org/10.1137/1035134

[9] A. Mitra, "Bit error analysis of new generation wireless transceivers," in *The 8th International Conference on Communication Systems*, vol. 2, 2002, pp. 636–640 vol.2.

[10] J. Allen, "Short term spectral analysis, synthesis, and modification by discrete fourier transform," *IEEE Transactions on Acoustics, Speech, and Signal Processing*, vol. 25, no. 3, pp. 235–238, 1977.

[11] H. Andrews and C. Patterson, "Singular value decomposition (SVD) image coding," *IEEE Transactions on Communications*, vol. 24, no. 4, pp. 425–432, 1976.

[12] K. Mishra, S. Kumar Singh, and P. Nagabhushan, "An improved SVD based image compression," in *2018 Conference on Information and Communication Technology (CICT)*, 2018, pp. 1–5.

[13] A. R., G. Xavier, H. V., N. Prasannan, R. Peter, and K. Soman, "GNU radio based control system," in *International Conference on Advances in Computing and Communications*, 2012, pp. 259–262.

[14] "The signal metadata format (SigMF), v0.0.2, jan. 8, 2019, https://sigmf.org."

[15] USRP hardware driver and usrp manual. Ettus Research. [Online]. Available: https://files.ettus.com/manual/page_configuration.html

[16] Invitation to the future. Yaesu. [Online]. Available: https://www.yaesu.com/pdf/System_Fusion_text.pdf

[17] M. Chiani and A. Elzanaty, "On the LoRa modulation for IoT: Waveform properties and spectral analysis," *IEEE Internet of Things Journal*, vol. 6, no. 5, pp. 8463–8470, Oct 2019.

[18] RF modules. HopeRF. [Online]. Available: https://www.hoperf.com/modules/lora/RFM98.html

[19] C. H. Taal, R. C. Hendriks, R. Heusdens, and J. Jensen, "A short-time objective intelligibility measure for time-frequency weighted noisy speech," in *2010 IEEE International Conference on Acoustics, Speech and Signal Processing*, 2010, pp. 4214–4217.

[20] V. Panayotov, G. Chen, D. Povey, and S. Khudanpur, "Librispeech: An ASR corpus based on public domain audio books," in *2015 IEEE International Conference on Acoustics, Speech and Signal Processing (ICASSP)*, 2015, pp. 5206–5210.